

# The reflectance modeling in shape from shading

L. Hashemi<sup>a\*</sup>, A. Azizi<sup>a</sup>, M. Rezaeian<sup>a</sup>  
Dept. of Geomatics Engineering, University of Tehran, Tehran, Iran  
(lhashemi, aazizi, mrezaeian)<sup>a</sup>@ut.ac.ir

Commission V, WG V/6

**KEY WORDS:** Photogrammetry, Radiometry, Modeling, Visualization, DEM/DTM, Radiation

## ABSTRACT:

Shape from Shading is one of the methods used for shape recovery which exploits the fact that surface patches, having different inclination relative to a light source are imaged with different brightness.

In order to solve the DTM reconstruction problem by SFS the image formation process has to be modeled and eventually inverted with respect to the parameters describing the object surface. Surface reflectance can be exactly described by its bi-directional distribution function (BRDF).

In this paper we show that there exist images that could not have arisen from shading on the smooth surface with uniform reflecting properties. This means that the gray shade values are also significantly influenced by the other factors, which have not been included into SFS functional model.

## 1. INTRODUCTION

### 1.1. Introduction

Shape recovery in computer vision is an inverse problem, which transforms single or stereo 2D images to a 3D scene. Shape from shading (SFS) is one of the methods used for shape recovery which exploits the fact that surface patches, having different inclination relative to a light source are imaged with different brightness. The surface is generally assumed to have constant and known reflectance properties. Therefore SFS only performs well in area with poor image texture where digital image matching fails to produce correct results.

### 1.2. Image formation

In order to solve the DTM reconstruction problem by SFS the image formation process has to be modeled and eventually inverted with respect to the parameters describing the object surface. The image gray values are influenced by the radiance and wavelength of incident illumination, atmospheric effects, surface reflectance properties and sensor characteristics.

Light fall onto the surface enclosing the incidence angle  $i$  between the direction to the light source  $\vec{s}$  and the local surface normal  $\vec{N}$ . The incoming irradiance  $E_0$  is partly absorbed and partly scattered back into upper hemisphere. A sensor lying in direction  $\vec{V}$ , which encloses the emittance angle  $e$  between  $\vec{V}, \vec{N}$  registers the radiance  $L$  scattered toward the sensor.

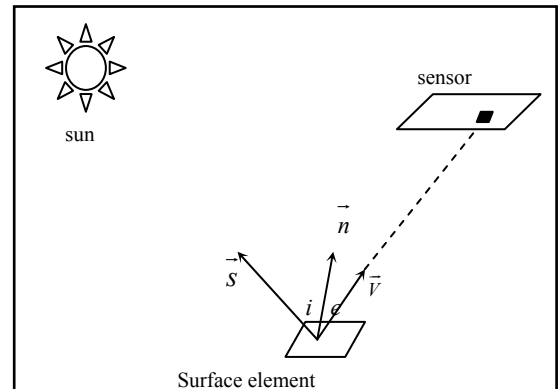


Figure 1. Principle of image formation

## 2. REFLECTANCE MODELS

Surface reflectance can be exactly described by its bi-directional distribution function (BRDF). This function describes how light from a given direction is reflected from a surface at a given orientation. In its full generality different spectra of light may be reflected in an orientation dependent way; thus, the BRDF may be, at least theoretically, very complex indeed.

## 2.1. Lambertian Reflectance Model

Lambertian surfaces are surfaces having only diffuse reflectance, i.e. surfaces which reflect light in all directions. The brightness of a Lambertian surface is proportional to the energy of the incident light. The amount of light energy falling on a surface element is proportional to the area of the surface element as seen from the light source position that is cosine function of the angle between the surface orientation and the light source direction ( $i$ ). Therefore the Lambertian surface can be modeled as the product of the strength of the light source  $E_0$ , the albedo of the surface  $A$  and the foreshortened area  $\cos i$  as follows:

$$I_l = E_0 A \cos i \quad (1)$$

Where  $I_l$  is the reflectance map (figure1). If the surface normal and the light source direction both are unit vector the above formula can be rewritten as:

$$I_l = E_0 A \vec{N} \cdot \vec{S} \quad (2)$$

Where “ $\cdot$ ” represents dot product.

Recent work by Wolff has demonstrated that the Lambertian model only really applies when the angle of incidence and the angle of reflection is small (relative to the surface normal). Importantly, Wolff has developed a simple modification of Lambert's law, which accurately accounts for all illumination and viewing directions.

## 2.2. Specular Reflectance Model

Specularity only occurs when the incident angle of the light source is equal to the reflected angle. It is formed by two components: the specular spike and the specular lobe.

The specular spike is zero in all directions except for a very narrow range around the direction of specular reflection.

The specular lobe spreads around the direction of specular reflection. The simplest model for specular reflection is described by the following delta function:

$$I_s = E_0 \delta(\theta_s - 2\theta_r) \quad (3)$$

Where  $I_s$  is the specular brightness,  $E_0$  is the strength of the specular component,  $\theta_s$  is the angle between the light source direction and the viewing direction and  $\theta_r$  is the angle between the surface normal and the viewing direction. This

model assumes that the highlight caused by specular reflection is only a single point, but in real life this assumption is not true.

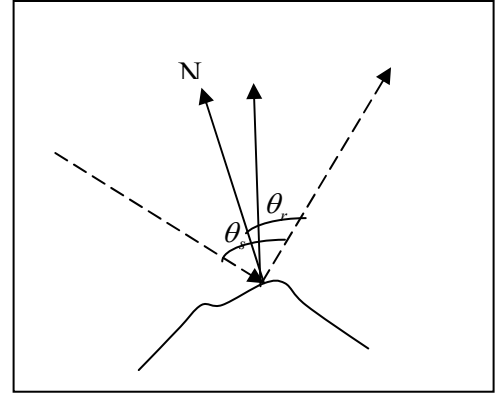


Figure 2. Sprcular reflection

## 2.3. Hybrid Reflectance Model

Most surfaces in the real world are neither purely Lambertian nor purely specular, they are a combination of both. That is, they are hybrid surfaces. One straightforward equation for a hybrid surface is:

$$I = (1 - \varpi)I_l + \varpi I_s \quad (4)$$

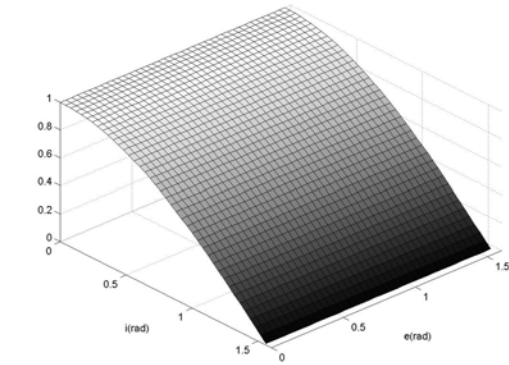
Where  $I$  is the total brightness for the hybrid surface,  $I_s, I_l$  are the specular brightness and Lambertian brightness, respectively, and  $\varpi$  is the weight of the specular component. One of the hybrid models that are used in photogrammetry is the Lommel-Seeliger that assumes the radiance observed at a sensor comes from light scattered by all particles in the medium lying within the field of view of the sensor. Therefore the Lommel-Seeliger law contains not only the incidence angle  $i$  but also the emittance angle  $e$ :

$$I_{ls} = 2E_0 A \frac{\cos i}{\cos i + \cos e} \quad (5)$$

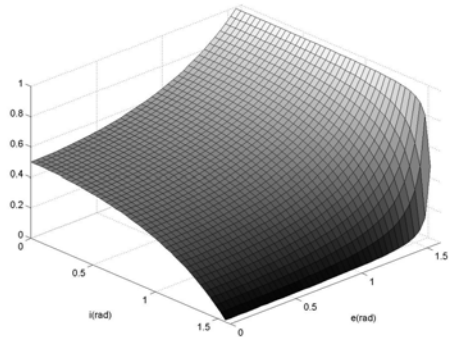
Where  $I_{ls}$  is the Lommel\_seeliger brightness. This law is a good description of the light scattering behaviour of low albedo surface. In the figure 3a ,3b the two reflectance models are depicted graphically with respect to the incidence and emittance angle. According to the figures and the equations, for the lommel-seeliger model for a vertical image of a horizontal

surface patch ( $e = 0$ ) with illumination directly from above ( $i = 0$ ),  $I_{ls}$  is only half the value of  $I_l$ .

Although the lambertian model is widely used because of its simplicity, it is a poor approximation to the diffuse component of rough surfaces.



(a)



(b)

Figure 3. (a) Lambertian model  
(b) Lommel-seeliger model

### 3. IMPLEMENTATION

A number of techniques have been developed for modeling object shapes by observing real objects. However, attempts to model reflectance properties of real objects have been rather limited. In most cases, modeled reflectance properties are too simple or too complicated to be used for synthesizing realistic images of the object. In this research work, the lambertian model is utilized for modeling the terrain reflectivity property. It is very difficult to choose good test image for SFS algorithms. A good test image must match the assumptions of the algorithms, e.g. lambertian reflectance model, constant albedo value. But there are some images that could not have arisen from shading on a smooth surface with uniform reflecting properties and lighting. It is not difficult to satisfy these assumptions for synthetic image. In real image, there will be errors to the extent that these assumptions are not matched. In this research, simulate data was generated using a predefined bilinear surface and for real data an aerial photograph of a smooth hilly terrain with low information content was chosen. Synthetic image in scale of 1:40000 was generated by a ray tracing algorithm, using the synthetic DTM, together with a constant value for the surface albedo. The exterior orientation of the image and light source position were considered as known values.

Also one black and white aerial image with an image scale of approximately 1:40000 of poorly texture area in Iran was used. The image was digitized using photogrammetric scanner with a pixel size of  $14\mu\text{m}$ , resulting in a ground sample resolution of about 0.56m. The interior and exterior orientation were determined using digital stereo plotter. The illumination direction was calculated from known time of the image acquisition and geographical coordinates of surface area.

In order to investigate of potential of the reflectance model, we consider the equal profiles on the DTM and image.

The correlation values for the slope and gray shade variation were obtained to assess the dependency between the gray shade variation and the slope variation for the real data. The correlation for these factors were small for the real data as compared with the simulated data (figure 4, figure 5). This means that gray shade values are also significantly influenced by the other factors such as non-uniform terrain albedo, atmosphere, etc. which have not been included into Lambertian model.

Also, one of the main reasons why modeling of reflectance properties has been unsuccessful, compared with modeling of object shapes, is that both diffusely reflected lights and specularly reflected lights, i.e., the diffuse and specular reflection components are treated together, and therefore, estimation of reflectance properties becomes unreliable. To eliminate this problem, the two reflection components should be separated prior to estimation of reflectance properties.

#### 4. CONCLUSION

The mathematical model for the SFS is established based on the fact that the pixel's gray level variations in image space are proportional to the shading intensity variations of the terrain morphology. The terrain shades in its turn is the function of the illumination intensity and the direction of the incident light with respect to the local surface orientation as well as the incident light direction and the terrain albedo. In this project the Lambertian model is utilized for modeling the terrain reflectivity property.

The result for the real image shows that the Lambertian reflection does not sufficiently describe surface reflectance properties. Surfaces with unknown and varying albedo must be considered.

There are several possible directions for future research. As we noted, reflectance models used in SFS methods are too simplistic; recently, more sophisticated models have been proposed. This not only includes more accurate models for Lambertian, specular, and hybrid reflectance, but also includes replacing the assumption of orthographic projection with perspective projection, which is a more realistic model of cameras in the real world.

#### 5. REFERENCE

Dupuis P., Oliensis J.; 1992. Direct Method for Reconstructing. *Pattern Recognition*, pp. 453-458.

L. Hashemi, A. Azizi, M. Hashemi; 2002. Implementation on a Single Photo Shape from Shading Method for the Automatic DTM Generation.

Heipke C., Piechullek C.; 1996. DTM Refinement Using Multi Image Shape from Shading. *IntArchPhRs*, (31), B3/III, pp. 644-651.

Heipke C., Piechullek C., Ebner H.; 2000. SIMULATION STUDIES AND PRACTICAL TESTS USING MULTI IMAGE SHAPE FROM SHADING. *IntArchPhRs*, Vol. XXXIII, B3, pp. 724-729.

Horn B.K.P.; 1970. Shape from Shading : A Method for Obtaining The Shape of a Smooth Opaque Object from one view. PhD Thesis, Department of Electrical Engineering, MIT.

Horn B.K.P.; 1990. Height and Gradient from Shading. *International Journal of Computer Vision*, (5) 1, pp. 37-75.

Horn B.K.P., Szeliski R.S., Yuille A.L.; 1993. Impossible Shaded Images. *IEEE Transactions on Pattern Analysis and Machine Intelligence*, Vol. 15, no. 2, pp. X6-170.

Piechullek C., Heipke C., Ebner H.; 1998. Multi Image Shape from Shading - RESULTS USING REAL AERIAL IMAGERY.

Zhang R., Tsai P.S., Cryer J.E., Shah M.; 1999. Shape from Shading : A Survey. *IEEE Transactions on Pattern Analysis and Machine Intelligence*, Vol. 21, no. 8, pp. 690-706.

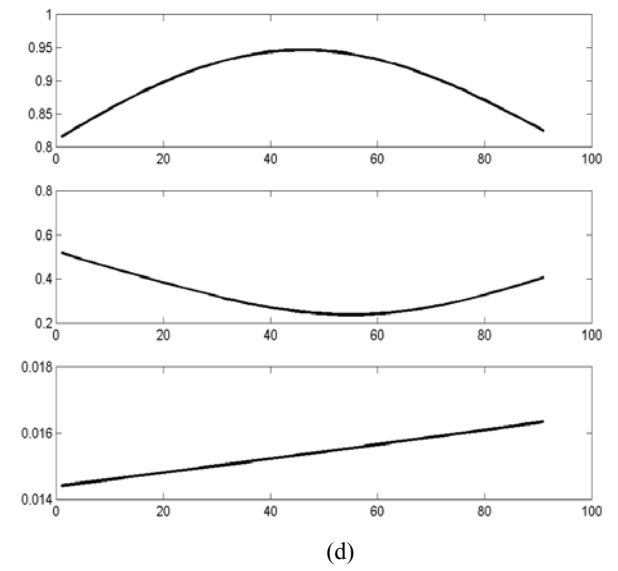
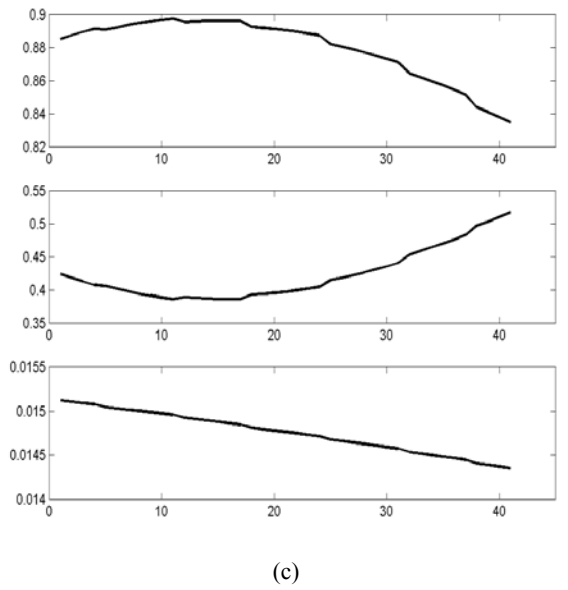
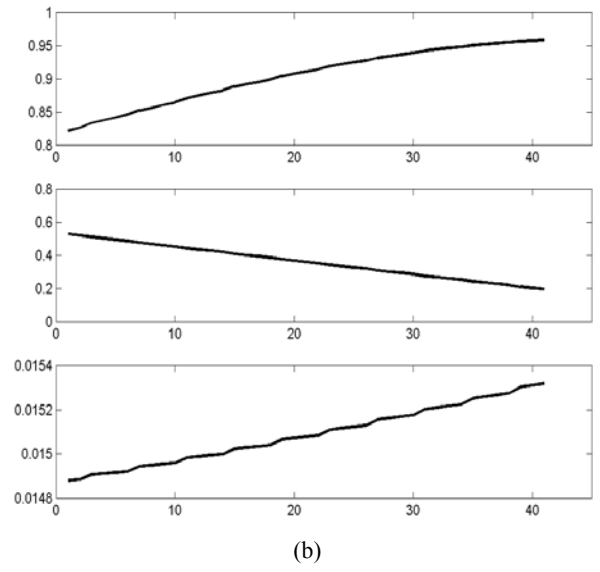
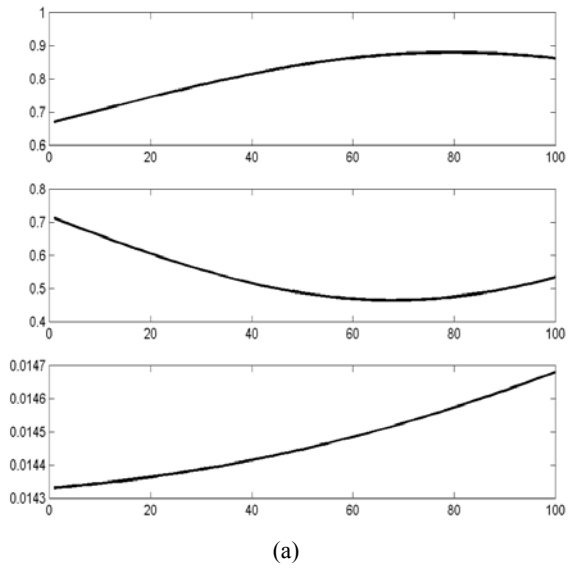


Figure 5. (a) , (b) , (c), (d) Correlation between slope variation and gray shade variation for synthetic image

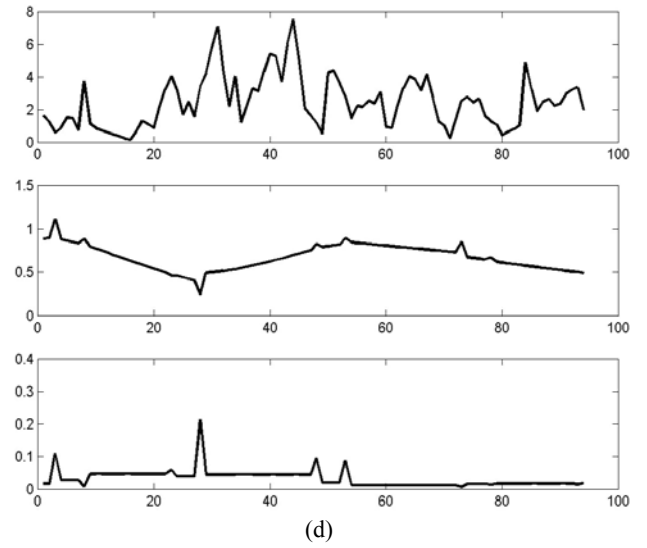
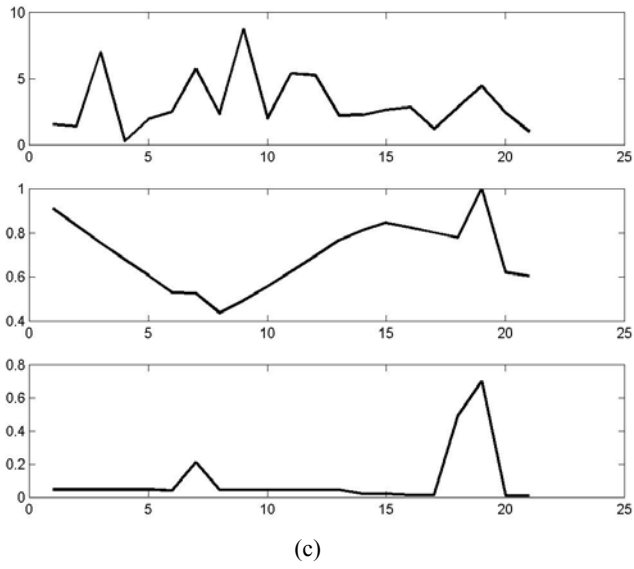
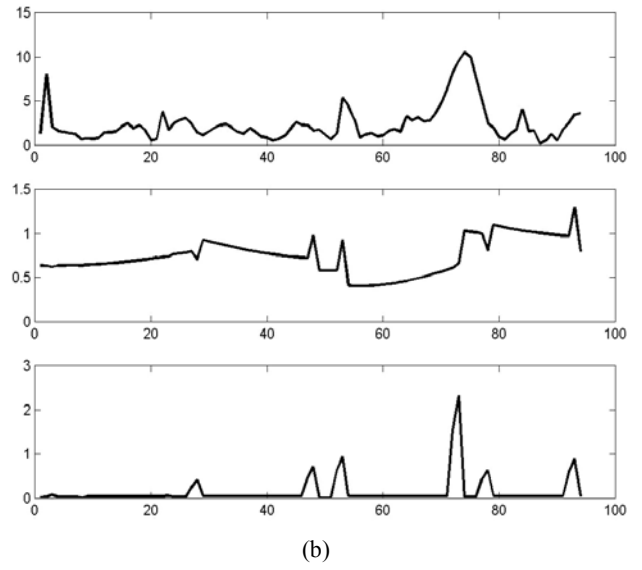
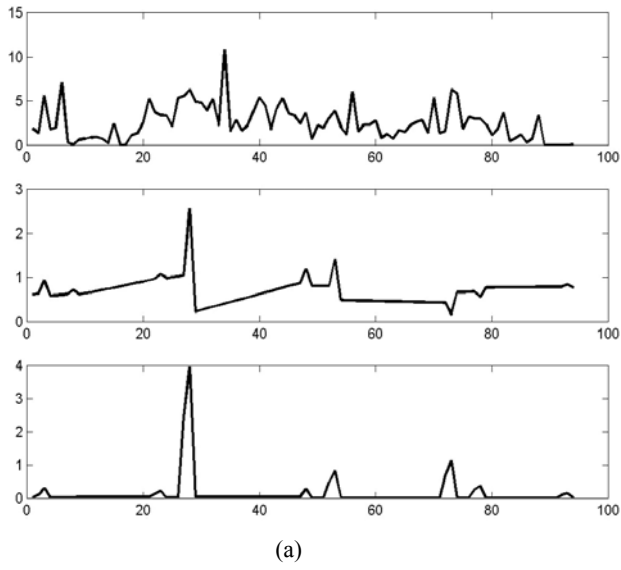


Figure 5. (a) , (b) , (c), (d) Correlation between slope variation and gray shade variation for real image